separations

MDPI

*Article*

# Production of Diol-Modified Column Packing Material and Its Use in Novel HPLC Method for Urea Analysis in Dialysis Process

**Murat Altan [1,2,3,*] and Uğur Şahin [1,2,3]**

[1] Faculty of Science, Department of Chemistry, Erciyes University, Kayseri 38039, Türkiye; ugurs@erciyes.edu.tr
[2] Nuri-Zekiye Has Institutes Building Science Institute, Erciyes University, Kayseri 38039, Türkiye
[3] USEM Research and Development Center, Incubation Center-1, Erciyes University Technology Development Zone, Kayseri 38039, Türkiye
* Correspondence: murat.altan@farmasol.com.tr

**Abstract**

Dialysis is a widely used and effective method for removing urea from protein solutions, particularly following protein denaturation or solubilization. Due to its small molecular weight (~60 Da), urea can pass through semipermeable membranes, while larger protein molecules are retained. Therefore, the performance of dialyzers in urea removal is critically important. Dialyzer performance is commonly evaluated according to the method specified in the ISO 8637-1 standard, which is based on the measurement of urea concentrations in aqueous solutions before and after dialysis. In this study, a novel diol-modified silica, typically used as a column packing material in HPLC, was synthesized and applied as a new column. Using this column, a new HPLC method combined with a refractive index detector (RID) was developed for the sensitive and accurate determination of urea in aqueous sample solutions. This study is the first to report quantitative urea analysis using a diol-modified column packing material. Method accuracy was evaluated through standard addition-recovery experiments. The method showed recovery values between 99 and 110%, a limit of detection (LOD) of 0.66 mg/L, a limit of quantification (LOQ) of 2.0 mg/L, and a relative standard deviation (RSD) of 4.4%.

**Keywords:** urea analysis; dialysis; diol-modified silica particles; high-performance liquid chromatography

## 1. Introduction

Dialysis is a treatment used to remove harmful substances and excess fluid from the blood when the kidneys are unable to perform their functions. Normally, the kidneys filter the blood, maintaining internal balance; however, this function can be impaired by certain diseases, kidney failure, or genetic factors [1,2]. Dialysis, which is used when the kidneys are insufficient, helps remove toxins and excess fluid from the body. This treatment, which has two main methods, hemodialysis and peritoneal dialysis, improves the patient's quality of life and contributes to the maintenance of vital functions. Dialysis is used to remove small unwanted molecules (e.g., salts, urea, detergents, or other denaturants) from a solution containing larger molecules like proteins or nucleic acids [3–5].

Urea is the most prevalent small-molecule metabolic waste product that must be eliminated during dialysis, whether utilizing a single-pass system or a regenerated dialysate system. Although the urea clearance rate is commonly used as a standard measure of dialysis effectiveness, it has important limitations. Specifically, urea kinetics do not accurately reflect the behavior of many other uremic retention solutes, and urea alone does not

Check for updates

Academic Editor: Rosanna Ciriello

Received: 13 April 2026
Revised: 23 May 2026
Accepted: 25 May 2026
Published: 10 June 2026

**Copyright:** © 2026 by the authors. Licensee MDPI, Basel, Switzerland. This article is an open access article distributed under the terms and conditions of the Creative Commons Attribution (CC BY) license.

account for the wide array of metabolic and clinical disturbances underlying the uremic syndrome [6,7].

Nevertheless, recent experimental evidence has indicated that urea can exert toxic effects at concentrations typically observed in chronic kidney disease (CKD). Urea has been shown to induce various molecular disruptions, including the promotion of insulin resistance, increased free radical production, initiation of apoptosis, and impairment of the intestinal barrier's protective function. Furthermore, urea contributes to the generation of harmful byproducts such as cyanate, ammonia, and carbamylated compounds [8,9]. Of particular concern are post-translational protein modifications caused by carbamylation, which have been implicated in atherosclerosis and other functional impairments. In clinical observational studies, the presence of carbamylated compounds has been consistently associated with increased cardiovascular risk, as well as higher overall morbidity and mortality [8–11].

There are several main methods aimed at urea purification, but each is based on slightly different physical principles. These methods are as follows: (1) hemodialysis (HD), (2) peritoneal dialysis (PD), (3) hemofiltration (HF), (4) hemodiafiltration (HDF) and (5) Continuous Renal Replacement Therapy (CRRT). Hemodialysis using dialyzers (artificial kidneys) is the most common method.

The urea removal ability of dialyzer filters used during dialysis serves as an indicator of process performance. Measuring urea levels in the spent dialysate allows for a direct calculation of the amount of urea removed during a single dialysis session. This measurement is referred to as true removed urea (TRU) [12–14].

While most existing methods for urea determination have traditionally targeted clinical applications [15,16], there is an increasing need for sensitive and reliable assays to measure urea in diverse matrices such as biological samples, dialysis solutions, milk, soil extracts, seawater, and wine [17–19]. Two primary techniques dominate both research and routine analyses:

1. **Hydrolysis**: This method uses urease to catalyze the breakdown of urea, followed by detecting the released ammonia via colorimetric or electrochemical methods [20].
2. **Non-Enzymatic Reaction**: Urea reacts directly with butane-2, 3-dione monoxime or similar reagents, producing colored compounds [21].

Each method, however, has limitations. Non-enzymatic approaches generate unpleasant odors and involve hazardous chemicals, limiting their desirability in clinical and winemaking contexts. Conversely, these methods are often preferred for environmental samples, where enzyme inhibitors or unsuitable conditions reduce the effectiveness of urease-based assays. Furthermore, many samples require extensive pre-treatment to eliminate interfering substances before either method can be applied.

High-performance liquid chromatography (HPLC) methods for urea analysis have also been explored [22,23], but their adoption remains limited due to procedural complexity and insufficient sensitivity. While urea is a small, highly polar molecule that can be challenging to analyze by conventional HPLC methods, specialized approaches have been developed.

This study presents the development of a novel high-performance liquid chromatography (HPLC) method designed for the precise and sensitive detection of urea in aqueous solutions. A new HPLC column was synthesized using diol-modified silica as the stationary phase. The developed method demonstrated high analytical performance, with an accuracy range of 99% to 110%, a limit of detection (LOD) of 0.66 mg/L, and a relative standard deviation (RSD) of 4.4%.

## 2. Materials and Methods

### *2.1. Materials and Reagents*

Urea standard (≥99.0%) was obtained from Sigma (Sigma-Aldrich, St. Louis, MO, USA), while Disodium hydrogen phosphate dihydrate, sodium dihydrogen phosphate dihydrate ethanol, methanol, acetonitrile, and toluene of analytical grade purity were purchased from Merck (Darmstadt, Germany). Deionized water (18.2 MΩ·cm) was produced using a Milli-Q system (Millipore, Burlington, MA, USA). 3-Aminopropyl triethoxysilane (3-APTES) was sourced from Fluorochem (Fluorochem Ltd., Hadfield, Derbyshire, UK), and ultrapure silica gel was acquired from Silicycle (SiliCycle Inc., Quebec City, QC, Canada). A urea stock solution at a concentration of 1000 mg/kg was prepared in a methanol/deionized water mixture (20:80, $v/v$) and subsequently diluted with acetonitrile for further experimental use. The determination of urea was carried out using a HPLC-DAD system by using a mobile phase composed of ultrapure water (component A) and acetonitrile (component B) in proportion (67:33, $v/v$). Therefore, urea stock solution was diluted with acetonitrile. For buffer preparation, 3.28 g of sodium dihydrogen phosphate dihydrate and 0.028 g of disodium hydrogen phosphate dihydrate were weighed and transferred into a 500 mL volumetric flask. The flask was filled to volume with ultrapure water, and the pH was adjusted to 5 using diluted hydrochloric acid and sodium hydroxide.

### *2.2. Instrumentation*

All devices and equipment used in the experimental stages and their purposes are summarized in Table 1. All instruments and equipment used in the experimental studies are given in Table 1. Chromatographic analyses were performed using an Agilent 1260 Infinity Series HPLC system equipped with a diol-modified silica column (Agilent Technologies, Santa Clara, CA, USA). The mobile phase was degassed with an ultrasonic stirrer prior to analysis. Characterization of the synthesized materials was performed using FT-IR and XRD analyses, and surface morphology was examined using FE-SEM. Structural verification was performed using NMR spectroscopy. Centrifugation was used in the sample preparation stage, and drying was performed in an oven. All weighings were performed using an analytical balance.

**Table 1.** All devices and equipment used in the experimental stages.

| Instrument/Tool | Model/Brand | Function/Application |
|---|---|---|
| HPLC System | Agilent 1260 Infinity Series (Agilent Technologies, Santa Clara, CA, USA) | Used for chromatographic separation of analytes using an in-house prepared amino column. |
| HPLC Column | Diol-modified silica particles filling column (250 mm × 4.6 mm, 5 µm) | Custom-made; utilized for effective separation during HPLC analysis. |
| Ultrasonic Mixer | Bandelin Sonorex (Bandelin electronic GmbH & Co. KG, Berlin, Germany) | Used to degas and homogenize the mobile phase by eliminating trapped gas bubbles. |
| FT-IR Spectrometer | Spectrum 400 with ATR unit (Waltham, MA, USA) | Used to obtain infrared spectra for functional group characterization of synthesized materials. |
| X-ray Diffraction (XRD) System | PANalytical Empyrean (Malvern, UK) | Employed to determine the crystalline structure of amino-modified silica particles. |
| Field Emission SEM (FE-SEM) | Zeiss Gemini-500 (Carl Zeiss AG, Oberkochen, Germany) | Used for morphological analysis and surface imaging of synthesized silica. |

**Table 1.** *Cont.*

| Instrument/Tool | Model/Brand | Function/Application |
| --- | --- | --- |
| Suspended State Proton NMR Spectrometer | Bruker Avance III, 400 MHz (Karlsruhe, Germany) | Applied for structural elucidation via nuclear magnetic resonance of synthesized compounds. |
| Centrifuge | Hettich Universal 320 (Andreas Hettich GmbH & Co. KG, Tuttlingen, Germany) | Utilized during sample preparation to separate solid and liquid phases. |
| Drying Oven | Memmert (Memmert GmbH + Co. KG, Schwabach, Germany) | Employed for drying the silica particles coated with diol functional groups. |
| Analytical Balance | Precisa LS 220 A SCS (Precisa Gravimetrics AG, Dietikon, Switzerland) | Used for precise weighing of all solid samples and reagents. |

### *2.3. Synthesis of Diol-Modified Silica Particles as Stationary Phase Material for HPLC Column*

In total, 70 mL of toluene was added to 2.0 g of commercially purchased dry silica particles and suspended using an ultrasonic mixer. In a separate beaker, 2.5 g of 3-glycidoxypropyltrimethoxysilane (3-GPTMS) and 15 mL of toluene were mixed and suspended in an ultrasonic mixer. The mixture was slowly added to the initial mixture. This mixture was thoroughly suspended, connected to a reflux condenser, and boiled for 2 h. After 2 h, the mixture was centrifuged at 3000 rpm for 4 min. The liquid solvent was discarded, and the diol-modified silica particles at the bottom were washed twice with 100 mL of toluene, twice with 100 mL of ethyl alcohol, twice with 100 mL of methyl alcohol, once with distilled water, and finally once with methyl alcohol. The mixture was stirred with 75 mL of 0.1 M HCl for 2 h and then washed with pure water until a neutral pH was achieved. Then, it was washed with 100 mL of methanol and the diol-modified silica gel particles were dried at 60 °C for 12 h in an oven.

### *2.4. Filling Procedure of HPLC Column with Diol-Modified Silica Gel Particles*

To begin the column packing process, 2.0 g of silica particles functionalized with diol were dispersed in 25 mL of methanol. The mixture underwent ultrasonic agitation for five minutes, ensuring complete homogenization of the suspension. This uniform slurry was then carefully introduced into the reservoir column. At the bottom of the reservoir, a stainless steel HPLC column (250 mm in length, 4.6 mm inner diameter, 5 µm particle size) was attached to allow downward packing. After sealing the reservoir, the entire assembly was connected to a high-pressure pump. The system was inspected for leaks or inconsistencies, and once its stability was confirmed, the packing procedure commenced under a pressure of approximately 250 bar. After the silica was successfully packed into the HPLC column, it was flushed with acetonitrile to remove any residual solvents or loosely bound material. Finally, the prepared column was integrated into the HPLC-DAD and HPLC-RID system, where it underwent a series of quality control tests to verify its performance and readiness for analytical applications.

### *2.5. Development of HPLC-DAD and HPLC-RID Methods for Urea Analysis*

The determination of urea was carried out using a HPLC-DAD system. A key component of the setup was the use of a custom-synthesized silica-based diol column (250 mm × 4.6 mm, 5 µm). Initially, a mobile phase composed of ultrapure water (component A) and acetonitrile (component B) in proportion (67:33, *v*/*v*) was employed to facilitate separation of urea from the matrix medium. The flow rate throughout the analysis was maintained at 0.5 mL/min. To identify the most suitable detection parameters for the

HPLC-DAD method, preliminary trials were conducted across multiple wavelengths 205, 215, and 254 nm to evaluate their effectiveness in capturing the urea signal with clarity and sensitivity. Among these, 205 nm emerged as the most favorable wavelength, providing optimal detection performance for urea. It was observed that when the HPLC-DAD system was used, the mobile phase and urea peaks could not be completely separated from each other and the peak symmetry was not uniform. Therefore, a method could not be developed using the DAD for urea analysis. The analytical performance parameters of DAD and RID were compared under optimum HPLC conditions for urea analysis. Consequently, analyses were checked with the RID under the optimum conditions. With the RID, a retention time of 2.510 min was obtained for urea. The urea and mobile phase peaks were completely distinguishable from each other and symmetrical peaks for urea were obtained using the HPLC-RID system.

### *2.6. Real Sample Applications*

The analytical performance of dialyzers employed in hemodialysis applications was assessed in accordance with the procedures defined in the International Organization for Standardization standard ISO 8637-1 [24]. This guideline evaluates dialyzer efficiency based on the removal of urea, determined by comparing urea concentrations in dialysis fluids before and after the dialysis process. During the present study, the ISO 8637-1 standard served as the principal reference for the determination of urea in dialyzer solutions. According to the standard, the test solution used for evaluating urea clearance should contain urea concentrations between 15 and 35 mmol/L, corresponding to approximately 0.90–2.10 g/L.

The accuracy of the developed HPLC-RID analytical procedure was investigated by analyzing urea concentrations in aqueous urea solutions prepared according to the ISO 8637-1 protocol. Initially, two dialyzer samples, identified as FR and PR, were examined in preliminary experiments. Following these initial assessments, recovery experiments were carried out by using urea model solutions which were prepared according to ISO 8637-1 standard.

For the standard addition/recovery analysis, known quantities of urea were added to the samples at four concentration levels: 30, 45, 60, and 90 mg/kg. The developed HPLC-DAD method was applied to these samples.

## 3. Results and Discussion

### *3.1. Characterization of Pure Silica and Diol-Modified Silica Particles*

Fourier-transform infrared (FT-IR) spectroscopy was employed to compare the spectral features of pure silica with those of diol-functionalized silica across the wavenumber range of 450–3950 $cm^{-1}$ (Figure 1). The spectra of silica exhibit characteristic bands associated with the vibrational modes of Si–O–Si and Si–OH groups, as previously documented in the literature [25]. Notably, the strong absorption band at 1072 $cm^{-1}$ corresponds to the asymmetric stretching vibrations of Si–O–Si linkages, reflecting the connectivity of silica tetrahedra through oxygen bridges in the three-dimensional network [25].

The FT-IR spectrum of the diol-modified silica further reveals pronounced alterations associated with the functionalization process. Distinct peaks at 971 $cm^{-1}$ and 1453 $cm^{-1}$ confirm the incorporation of diol groups into the silica surface. The band at 972 $cm^{-1}$ reflects changes in the silica environment attributable to the condensation of terminal silanol groups or the formation of covalent linkages with 3-GPTMS molecules during modification [26]. Meanwhile, the weak absorption near 3425 $cm^{-1}$ is characteristic of deformation vibrations of surface-bound –OH groups, providing strong evidence for the successful immobilization of diol functionalities. The presence of these bands also suggests the development of a partially ordered structure, likely shaped by hydrogen bonding or

additional surface interactions. Collectively, these spectral features serve as key indicators of the efficiency of the modification procedure and the resulting structural and functional behavior of the synthesized materials (Figure 1).

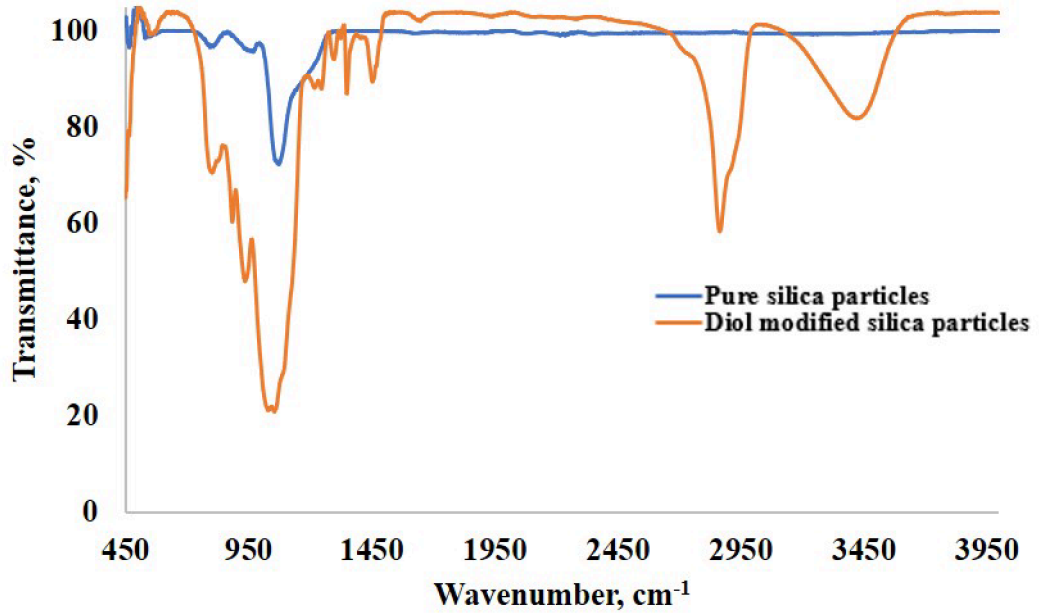



**Figure 1.** FTIR spectrum of pure silica particles and diol-modified silica particles.

The suspended $^{1}$H NMR spectrum of the diol-modified silica material in DMSO-D6 solution is presented in Figure 2. The chemical shifts corresponding to the aliphatic –$CH_2$– protons of diol-modified silica particles. Additionally, a distinct signal at 4.71 ppm, assigned to the free –OH group, provides further evidence that the diol functionality remains intact following the modification procedure, thereby enabling potential subsequent chemical functionalization. These resonances signify that the aliphatic chain is covalently anchored to the silica surface, reflecting the influence of the electronegative siloxane and diol groups that constitute the modified surface layer.

The X-ray diffraction (XRD) pattern of the pure and diol-modified silica, shown in Figure 3, clearly reflects the structural implications of the surface-level chemical modifications. Relative to the diffraction profile of unmodified silica, the broad feature typically observed between 2θ = 22–25° exhibits a marked decrease in intensity and a reduction in definition. Such changes indicate partial disruption of the amorphous silica matrix, arising from the substitution of surface silanol (–Si–OH) groups with diol functionalities during the modification process. Although the incorporation of diol groups maintains the overall amorphous character of the material, it induces localized structural perturbations that account for the diminished peak intensity.

Additionally, a distinct reflection at 2θ = 28.3° appears in the diol-modified silica spectrum. This peak is attributed either to the spatial organization of the grafted diol groups on the silica surface or to interactions between the organic moieties and the underlying silica network. The presence of this feature suggests that surface functionalization introduces new structural regularities as a direct consequence of the bonding environment created during modification. Collectively, these observations confirm the successful execution of the modification procedure and the effective incorporation of diol groups into the silica surface.

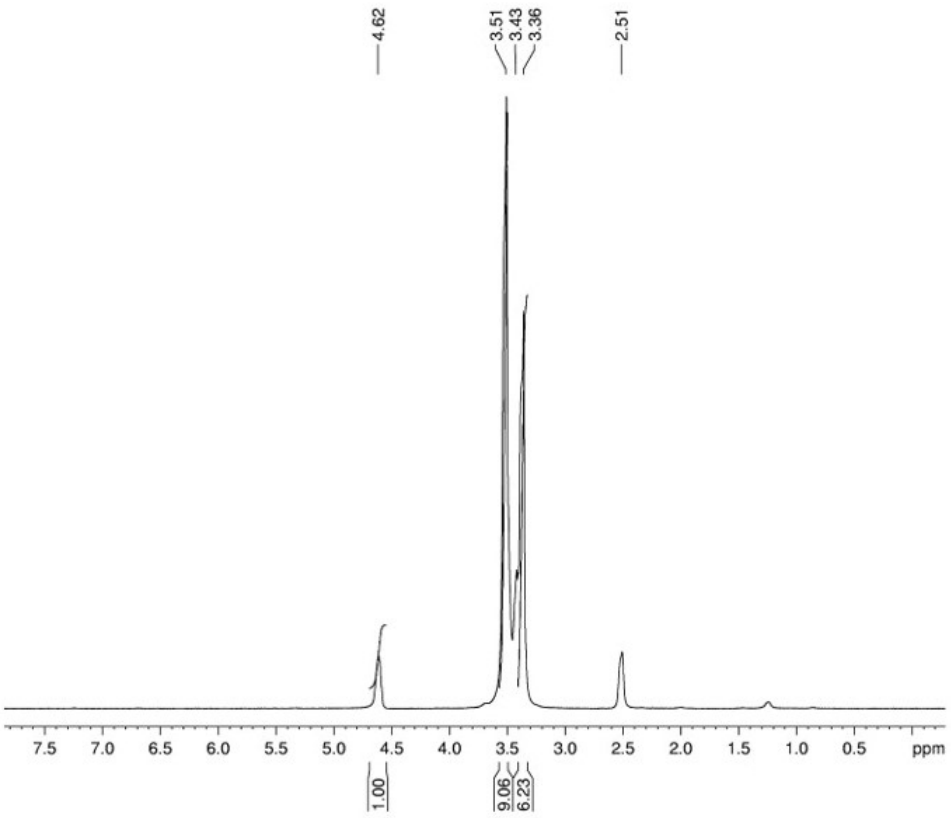



**Figure 2.** H-NMR spectrum of diol-modified silica particles in DMSO-D6 solution.

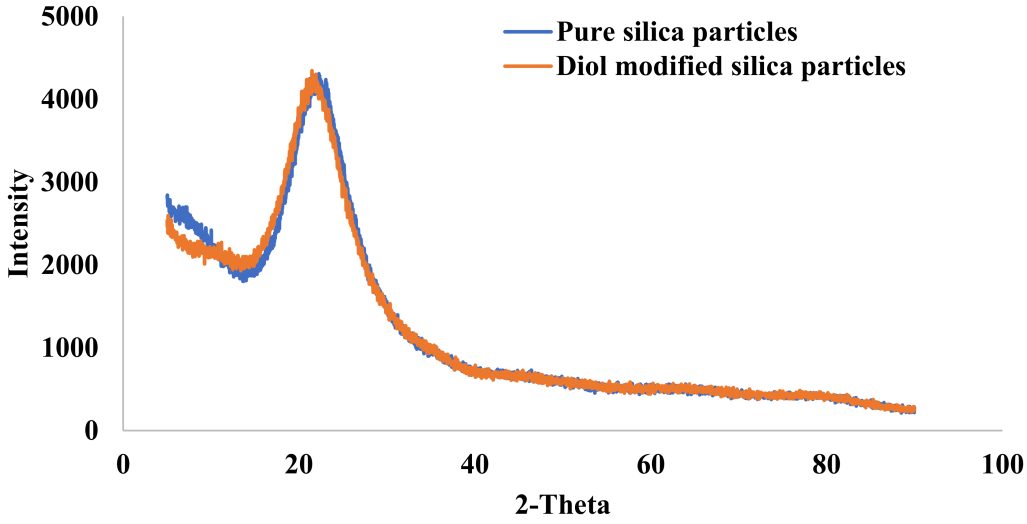



**Figure 3.** XRD spectrum of pure silica particles and diol-modified silica particles.

Field-emission scanning electron microscopy (FE-SEM) was employed to evaluate the differences in surface morphology between unmodified silica and diol-modified silica particles (Figure 4A–C). As shown in micrographs A and B, the pristine silica exhibits a predominantly spherical morphology with smooth, homogeneous surfaces and an average particle diameter of approximately 4.337 μm, consistent with its monodisperse character.

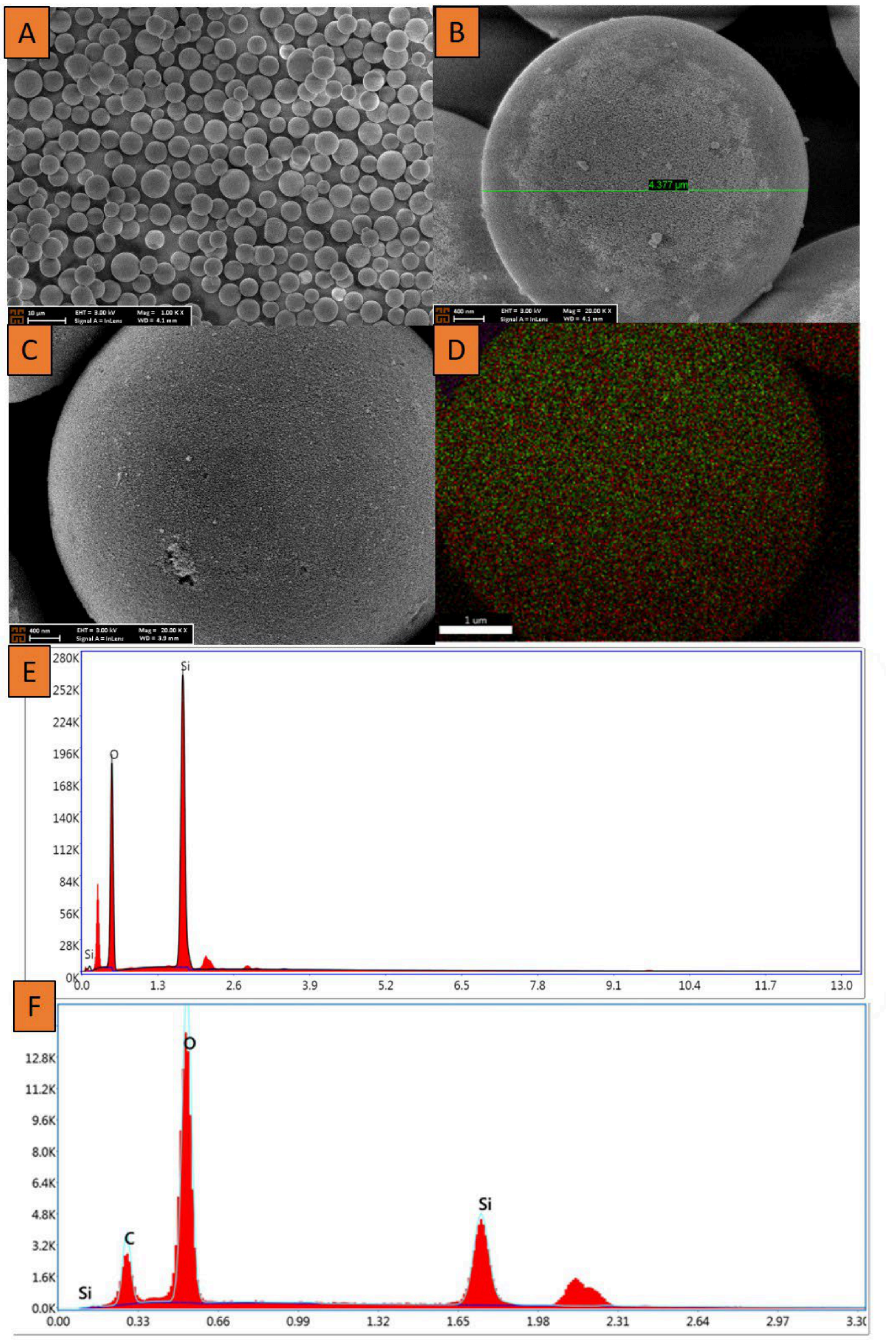



**Figure 4.** FE-SEM images of the pristine silica (**A**,**B**), FE-SEM images of the diol-modified silica particles (**C**), SEM-mapping image of the diol-modified silica particles (**D**), SEM-EDX spectrum of pristine silica (**E**) and SEM-EDX spectrum of diol-modified silica particles (**F**).

Following surface modification, the particles depicted in micrographs in Figure 4C largely retained their spherical shape; however, notable alterations in surface texture were observed. Specifically, the modified particles display increased surface roughness and a slight enlargement in average particle size to roughly 5.0 µm. These morphological changes are attributed to the introduction of diol groups, which generate localized irregularities in both surface roughness and particle distribution. Despite these modifications, the overall morphology of the silica particles remains well preserved.

The structural variations evident in Figure 4 therefore indicate that the surface chemistry of the modified silica has been significantly altered relative to the pure material.

Such modifications enhance the suitability of the diol-functionalized silica for targeted surface reactions.

The elemental composition of the diol-modified silica particles, as determined by FE-SEM Mapping and FE-SEM-EDS analysis, reveals oxygen, carbon and silicon contents of 57 wt%, 12 wt% and 30 wt%, respectively (Figure 4E). Elemental mapping further confirms a uniform distribution of oxygen, carbon and silicon across the particle surfaces (Figure 4D). Collectively, these observations confirm the effective attachment of diol groups to the silica surface, resulting in the introduction of new functional moieties and significant alterations in the surface chemistry of the modified material.

### *3.2. Optimization of Experimental Parameters in HPLC Analysis*

The selection of a detector combined with HPLC for the analyte to be determined is extremely important to ensure that mobile phase components do not interfere with the analyte and that reproducible results are obtained. Analyses were performed with both a refractive index detector (RID) and a diode array detector (DAD) to obtain accurate and reproducible urea analysis. For the DAD, analyses were performed at a flow rate of 1 mL/min at wavelengths of 205, 215, and 254 nm, respectively. While no peak for urea was obtained at a wavelength of 254 nm, 343.3 mAU·s and 507.5 mAU·s were obtained in the analyses at wavelengths of 215 nm and 205 nm, respectively. After reviewing the results obtained, we decided to continue the analyses at a wavelength of 205 nm.

The effect of mobile phase component ratios on urea analysis was systematically evaluated using the HPLC-DAD system. Evaluation parameters included peak area, peak height, and peak symmetry, the results of which are summarized in Table 2. The highest peak area (277.462 mAU) at 205 nm wavelength was observed when the mobile phase consisted of water and acetonitrile in a 33:67 ($v/v$) ratio, indicating maximal detection sensitivity for the analyte. Similarly, the peak height reached its maximum value (8.349 mAU) under this condition, reflecting improved separation and precise analyte detection. At this rate and with a 4.337 min retention time, the peak width was 0.6624.

**Table 2.** Effect of mobile phase component ratios on urea analysis.

| Mobile Phase Ratio, % (Water-Acetonitrile) | Flow Rate, mL/min | Injection Volume, µL | Wavelength, nm | Ret.Time, min | Width, min | Area, mAU·s | Height, mAu |
|---|---|---|---|---|---|---|---|
| 67-33 | 1.0 | 20 | 205 | 1.934 | 0.0764 | 35.834 | 6.702 |
| 67-33 | 1.0 | 20 | 215 | 1.913 | 0.1033 | 33.415 | 4.795 |
| 67-33 | 1.0 | 20 | 254 | Not detected | - | - | - |
| 50-50 | 1.0 | 20 | 205 | 1.972 | 0.1896 | 97.183 | 7.382 |
| 50-50 | 1.0 | 20 | 215 | Not detected | - | - | - |
| 50-50 | 1.0 | 20 | 254 | Not detected | - | - | - |
| 33-67 | 1.0 | 20 | 205 | 4.337 | 0.4731 | 277.462 | 8.233 |
| 33-67 | 1.0 | 20 | 215 | Not detected | - | - | - |
| 33-67 | 1.0 | 20 | 254 | Not detected | - | - | - |

The peak width at this ratio was 0.6624. In contrast, alternative mobile phase ratios produced asymmetric peaks and lower peak areas, demonstrating suboptimal chromatographic performance (Table 2).

The 33:67 ($v/v$) ratio achieved an optimal balance between the polarity of the water and the apolarity of acetonitrile for urea. Increasing the proportion of acetonitrile accelerated elution and increased both peak area and height, whereas lower acetonitrile content led

to delayed elution and distorted peak shapes. It was observed that as the amount of acetonitrile in the mobile phase composition increased, the retention time of urea shifted from 1.934 min to 4.337 min. The retention time under the optimized conditions was 4.337 min, which represents an ideal compromise between analysis speed and separation efficiency. Ratios producing longer retention times unnecessarily prolonged the analysis, while shorter retention times compromised separation quality.

Therefore, the mobile phase composed of water and acetonitrile in a 33:67 (*v*/*v*) ratio was determined to provide the most favorable combination of sensitivity, peak symmetry, and analytical accuracy for urea quantification (Table 2).

In the present study, this developed method focuses not on separating different species within a matrix, but only on the separation and analysis of urea. An isocratic elution system was preferred because satisfactory chromatographic separation was achieved under optimized isocratic conditions. In addition, the use of isocratic elution offers several practical advantages, including simpler method operation, improved reproducibility, reduced equilibration time between runs, and lower solvent consumption.

In HPLC-based analytical techniques, mobile phase flow rate is a crucial parameter. The effect of flow rate on both retention and peak area was investigated. For this purpose, studies were conducted at flow rates of 0.5 and 1 mL/min. At a flow rate of 0.5 mL/min, the retention time of urea was 4.42 min and the resulting peak area was 361.2 mAU·s, while at a flow rate of 1.0 mL/min, the retention time of urea was 2.18 min and the resulting peak area was 277.5 mAu·s. Further studies were conducted at a flow rate of 0.5 mL/min (Table 3).

**Table 3.** Effect of mobile phase flow rates on urea analysis.

| Mobile Phase Ratio, % (Acetonitrile-Water) | Flow Rate, mL/min | Injection Volume, µL | Wavelength, nm | Ret.Time, min | Width, min | Area, mAu·s | Height, mAu |
|---|---|---|---|---|---|---|---|
| 33-67 | 1.0 | 20 | 205 | 4.337 | 0.4731 | 277.462 | 8.233 |
| 33-67 | 1.0 | 20 | 215 | Not detected | - | - | - |
| 33-67 | 1.0 | 20 | 254 | Not detected | - | - | - |
| 33-67 | 0.5 | 20 | 205 | 4.42 | 0.6624 | 361.214 | 8.349 |
| 33-67 | 0.5 | 20 | 215 | Not detected | - | - | - |
| 33-67 | 0.5 | 20 | 254 | Not detected | - | - | - |

A calibration curve graph for urea was created under optimum conditions by using the HPLC-DAD system. For this purpose, urea standard solutions ranging from 25 mg/L to 200 mg/L were prepared and analyses were performed. The calibration curve equation obtained with a correlation coefficient ($R^2$) of 0.9876 is in the form of y = 1.2073x + 21.565.

The correlation coefficient ($R^2$) shows that the peak field signals obtained in response to increasing urea concentration do not increase linearly. In addition to these results, it was observed that the mobile phase and urea peaks could not be completely separated from each other and that the peak symmetry was not uniform for the HPLC-DAD analysis. Therefore, a method could not be developed using the DAD for urea analysis. Consequently, analyses were checked with the RID under the optimum conditions. With the RID, a retention time of 2.510 min was obtained for urea with 1 mL/min flow rate. The urea and mobile phase peaks were completely distinguishable from each other and symmetrical peaks for urea were obtained using the HPLC-RID system. Therefore, urea analysis for subsequent experiments was performed using an HPLC-RID system.

### *3.3. Analytical Performance Parameters for the Developed HPLC-RID Method*

Urea quantification was performed with the HPLC-RID analysis system, which was established as the optimal system. Separation was achieved using a column packed with diol-modified silica particles. To evaluate the analytical performance of the method, a calibration curve was constructed to determine key parameters, including the linear range, limit of detection (LOD), limit of quantification (LOQ), and correlation coefficients, under the optimized chromatographic conditions.

For calibration, eight standard solutions of urea were prepared at concentrations changing from 10 to 200 mg/L and analyses were performed. The calibration curve equation obtained with a correlation coefficient ($R^2$) of 0.997 is in the form of y = 1964.888x + 203.908. The resulting calibration curve demonstrated a strong linear relationship between concentration and detector response. The linear regression equation and the corresponding correlation coefficient ($R^2$) confirm the reliability and accuracy of the method across the tested concentration range.

To determine the limit of detection (LOD), the method was applied to ten standard solutions prepared at the lowest concentration of urea that could be measured accurately and reproducibly. The LOD was calculated using the following formula: three times the standard deviation of the peak areas obtained from these ten analyses, divided by the slope of the calibration curve. The limit of quantification (LOQ) was subsequently calculated by multiplying the LOD by a factor of 3.3. LOD and LOQ values were found to be 0.66 mg/L and 2.0 mg/L, respectively.

Method repeatability was expressed as the relative standard deviation (RSD, %) and evaluated by applying the developed HPLC-RID procedure to ten standard solutions containing 15 mg/L urea. The RSD value was found to be 4.4%. The results confirmed the precision and reliability of the method under the optimized analytical conditions.

### *3.4. Accuracy of the HPLC-RID Method for Real Sample Analysis*

The performance of dialyzers used in dialysis procedures is checked according to the method specified under the "ISO 8637-1" directive. The directive is based on the urea removal performance of dialyzers by the urea concentration in aqueous solutions before and after dialysis. The "ISO 8637-1 Extracorporeal systems for blood purification—Part 1: Haemodialysers, haemodiafilters, haemofilters and haemoconcentrators" standard was used as a reference when performing dialyzer urea analysis. According to this standard, the solution to be used when determining the urea separation of the dialyzer contains urea in the range of 15–35 mmol/L. This corresponds to a urea solution of 0.90–2.10 g/L. The accuracy of the developed HPLC-RID method was evaluated through analyses of the urea concentration in aqueous solutions by using the ISO 8637-1 directive. In this study, two different dialyzer samples coded as FR and PR were initially tested. Based on these preliminary trials, recovery studies were subsequently conducted on these samples.

In the standard addition-recovery experiments, urea standards were spiked into samples at four concentration levels: 30, 45, 60, and 90 mg/kg. The corresponding data for spiked and measured concentrations are summarized in Table 4. Recovery rates at the spiked levels of 30, 45, 60, and 90 mg/kg ranged from 100% to 102% for sample FR, and from 99% to 110% for sample PR. These results indicate that the developed HPLC-RID method satisfies quality control criteria in terms of accuracy and reliability, demonstrating its robustness and capacity to deliver precise and consistent measurements across different concentration levels.

**Table 4.** Standard addition and recovery results for aqueous urea solutions ($N = 3$).

| Samples | Added, (mg/kg) | Found, (mg/kg) | Recovery, (%) |
|---|---|---|---|
| FR | 30 | 30.0 ± 0.2 [a] | 100 |
| | 45 | 45.0 ± 2.1 | 100 |
| | 60 | 60.0 ± 2.0 | 100 |
| | 90 | 92.2 ± 2.2 | 102 |
| PR | 30 | 30.6 ± 1.9 [a] | 103 |
| | 45 | 45.0 ± 1.7 | 99 |
| | 60 | 66.6 ± 0.4 | 110 |
| | 90 | 97.1 ± 1.1 | 107 |

a: Mean ± standard deviation.

## 4. Conclusions

In this study, a silica-based diol column packing material, exhibiting performance comparable to that of many commercially available columns, was successfully developed and applied for the analysis of urea in aqueous solutions. The material was comprehensively characterized using FT-IR, XRD, $^1$H NMR, FE-SEM, and EDX techniques, confirming its structural and functional properties. The developed and optimized HPLC-RID method demonstrated excellent analytical performance, with recovery rates ranging from 99% to 110, a correlation coefficient ($R^2$) of 0.997, and a limit of detection (LOD) of 0.66 mg/kg. The method also exhibited satisfactory precision, as indicated by the calculated relative standard deviation (RSD) for urea of 4.4%.

A key objective of this study was to develop a column material offering cost advantages over existing commercial alternatives. The silica-based diol column achieved this goal, demonstrating strong industrial potential by reducing costs by approximately 30–40% relative to commercially available columns. Beyond its immediate application in urea determination, the developed material provides a versatile platform for the analysis of other diol-containing compounds across diverse matrices.

Looking forward, this work lays the groundwork for the next generation of cost-efficient and application-specific chromatographic materials. Future research will focus not only on expanding the analyte scope but also on tailoring surface functionalities to enhance selectivity and durability under varying analytical conditions. In addition, scaling up the production process and integrating the material into automated and high-throughput analytical systems could further strengthen its industrial relevance. Ultimately, such advancements may contribute to more accessible, sustainable, and widely deployable analytical solutions in clinical, environmental, and pharmaceutical fields.

**Author Contributions:** Conceptualization, M.A. and U.Ş.; methodology, M.A. and U.Ş.; validation, M.A. and U.Ş.; formal analysis, M.A. and U.Ş.; investigation, M.A. and U.Ş.; resources, M.A. and U.Ş.; data curation, M.A. and U.Ş.; writing—original draft preparation, M.A. and U.Ş.; writing—review and editing, M.A. and U.Ş.; visualization, M.A. and U.Ş.; supervision, U.Ş.; project administration, M.A. and U.Ş.; funding acquisition, M.A. and U.Ş. All authors have read and agreed to the published version of the manuscript.

**Funding:** Erciyes University Scientific Research Projects Unit (BAP) Project: FDK-2022-11747.

**Data Availability Statement:** The original contributions presented in this study are included in the article. Further inquiries can be directed to the corresponding author.

**Acknowledgments:** The authors would like to thank Erciyes University Scientific Research Projects Unit (BAP) for supporting this Project: FDK-2022-11747.

**Conflicts of Interest:** The authors declare no conflict of interest.

## References


1. Locatelli, F.; Buoncristiani, U.; Canaud, B.; Kohler, H.; Petitclerc, T.; Zucchelli, P. Dialysis Dose and Frequency. *Nephrol. Dial. Transplant.* **2005**, *20*, 285–296. [CrossRef]
2. Daugirdas, J.T.; Blake, P.G.; Ing, T.S. *Handbook of Dialysis*; Lippincott Williams & Wilkins: Philadelphia, PA, USA, 2025.
3. Kang, X.; Zhang, Y.; Sun, C.; Zhang, J.; Che, Z.; Zang, J.; Zhang, R. Effectiveness of Virtual Reality Training in Improving Outcomes for Dialysis Patients: Systematic Review and Meta-Analysis. *J. Med. Internet. Res.* **2025**, *27*, e58384. [CrossRef]
4. Klein, K.R.; Lingvay, I.; Tuttle, K.R.; Flythe, J.E. Glycemic Management and Individualized Diabetes Care in Dialysis-Dependent Kidney Failure. *Diabetes Care* **2025**, *48*, 164–176. [CrossRef]
5. Pyne, L.; Rossignol, P.; Giles, C.; Junek, M.; Mark, P.B.; Gallagher, M.; De Zoysa, J.R.; Devereaux, P.J.; Walsh, M. Safety and Efficacy of Steroidal Mineralocorticoid Receptor Antagonists in Patients with Kidney Failure Requiring Dialysis: A Systematic Review and Meta-Analysis of Randomised Controlled Trials. *Lancet* **2025**, *406*, 811–820. [CrossRef] [PubMed]
6. Daugirdas, J.T. Kinetic Modeling Programs for Hemodialysis Adequacy Focusing on Urea, Creatinine, Phosphate, and Beta-2-Microglobulin. *Semin. Dial.* **2025**, *38*, 161–165. [CrossRef]
7. Flythe, J.E. Dialysis—Reply. *JAMA* **2025**, *333*, 1546. [CrossRef] [PubMed]
8. Glorieux, G.; Burtey, S.; Evenepoel, P.; Jankowski, J.; Koppe, L.; Masereeuw, R.; Vanholder, R. A Guide to Uraemic Toxicity. *Nat. Rev. Nephrol.* **2026**, *22*, 50–68. [CrossRef]
9. Guo, M.; Ni, L.; Wu, X. Natural Products as Potential Therapeutic Candidates for Diabetic Kidney Disease: Molecular Mechanisms, Translational Challenges, and Future Prospects. *Int. J. Mol. Sci.* **2025**, *26*, 11637. [CrossRef] [PubMed]
10. García, F.M.; Quesada, V.E. CKD as a Cardiovascular Risk Factor. In *Blood Pressure Disorders in Acute and Chronic Kidney Diseases*; Berbari, A.E., Mancia, G., Redon, J., Eds.; Springer Nature: Cham, Switzerland, 2025; pp. 215–258, Updates in Hypertension and Cardiovascular Protection.
11. Tsang, Y.P.; Aryeh, K.S.; Wang, K.; Himmelfarb, J.; Yeung, C.K.; Kelly, E.J. Enhancing Therapeutic Strategies and Drug Development for Patients with Kidney Disease. *Expert Opin. Drug Saf.* **2026**, *25*, 23–48. [CrossRef]
12. Canaud, B.; Lucena, R.; Ward, R. Water and Dialysis Fluid Purity for Contemporary Hemodialysis. *Semin. Dial.* **2025**, *38*, 12–24. [CrossRef]
13. Chu, K.; Li, P.; Ausri, I.; Cañizares, B.; Vasconez, C.; Guo, Z.; Tang, X. A Two-Filter Adaptation to Achieve Enhanced Hemodialysis Performance. *Kidney Dial.* **2025**, *5*, 52. [CrossRef]
14. Sun, S.; Li, Y.; Zhi, L.; Zhao, W.; Zhao, C. Blood Purification Membranes Used in Liquid–Liquid Environments. In *Blood Purification Materials*; Zhao, C., Ed.; Royal Society of Chemistry: London, UK, 2025; pp. 101–124.
15. Xu, Z.; Yue, Y.; Xu, M.; Qian, L.; Dou, L. The Role of Cut-off Values for Creatinine, Blood Urea Nitrogen, and Uric Acid in Prognostic Assessment of Chronic Heart Failure: A Retrospective Cohort Study. *BMC Cardiovasc. Disord.* **2025**, *25*, 209. [CrossRef]
16. Paulus, M.C.; Melchers, M.; Van Es, A.; Kouw, I.W.K.; Van Zanten, A.R.H. The Urea-to-Creatinine Ratio as an Emerging Biomarker in Critical Care: A Scoping Review and Meta-Analysis. *Crit. Care* **2025**, *29*, 175. [CrossRef]
17. Charvadeh, S.R.; Ghalibafan, J.; Abbasi, A.; Haidary, A.; Salimi, E. Utilization of the Dialysate to Characterize Dialysis Adequacy by Using Microwave Urea Biosensor Based on Complementary Split-Ring Resonator (CSRR). *Measurement* **2025**, *241*, 115703. [CrossRef]
18. Mangwe, M.C.; Mason, W.A.; Reed, C.B.; Spaans, O.K.; Pacheco, D.; Bryant, R.H. A Systematic Review and Meta-Analysis of Cow-Level Factors Affecting Milk Urea Nitrogen and Urinary Nitrogen Output under Pasture-Based Diets. *J. Dairy Sci.* **2025**, *108*, 579–596. [CrossRef] [PubMed]
19. Simonyan, K.; Tsokolakyan, A.; Buniatyan, V.; Badasyan, A.; Yeranosyan, M. Urea Detection in Phosphate Buffer and Artificial Urine: A Simplified Kinetic Model of a pH-Sensitive EISCAP Urea Biosensor. *Sensors* **2025**, *25*, 6596. [CrossRef] [PubMed]
20. Chen, J.; Liang, M.; Wang, Z.; Ma, X.; Liu, J.; Zhuang, W.; Liu, D.; Zhao, A.; Lv, Y.; Cai, Y.; et al. Mechanism Analysis of NaOH-Urea Binary Low-Temperature High-Solid Pretreatment of Corn Stover and Application in Cellulosic Ethanol Production. *Biomass Bioenergy* **2025**, *203*, 108308. [CrossRef]
21. Kumar, P.; Ramulu Lambadi, P.; Kumar Navani, N. Non-Enzymatic Detection of Urea Using Unmodified Gold Nanoparticles Based Aptasensor. *Biosens. Bioelectron.* **2015**, *72*, 340–347. [CrossRef]
22. Koebel, M.; Elsener, M. Determination of Urea and Its Thermal Decomposition Products by High-Performance Liquid Chromatography. *J. Chromatogr. A* **1995**, *689*, 164–169. [CrossRef]
23. Philbert, S.A.; Church, S.J.; Unwin, R.D.; Cooper, G.J.S. Elevated Urea Levels in Human Frontotemporal Dementia and Amyotrophic Lateral Sclerosis *Post-Mortem* Brain Tissue: Evidence of a Multi-Dementia Pathogenic Mechanism. *bioRxiv* **2025**. [CrossRef]
24. *ISO 8637-1:2024*; Extracorporeal Systems for Blood Purification Part 1: Haemodialysers, Haemodiafilters, Haemofilters and Haemoconcentrators. ISO: Geneva, Switzerland, 2024.

25. Barbosa, S.; Ottone, M.; De Almeida, M.; Lage, G.; Almeida, M.; Nelson, D.; Dos Santos, W.; Clososki, G.; Lopes, N.; Klein, S.; et al. Ketalization of Ketones to 1,3-Dioxolanes and Concurring Self-Aldolization Catalyzed by an Amorphous, Hydrophilic $SiO_2$-$SO_3H$ Catalyst under Microwave Irradiation. *J. Braz. Chem. Soc.* **2018**, *29*, 1663–1671. [CrossRef]
26. Zhang, D.; Hegab, H.E.; Lvov, Y.; Dale Snow, L.; Palmer, J. Immobilization of Cellulase on a Silica Gel Substrate Modified Using a 3-APTES Self-Assembled Monolayer. *SpringerPlus* **2016**, *5*, 48. [CrossRef] [PubMed]

**Disclaimer/Publisher's Note:** The statements, opinions and data contained in all publications are solely those of the individual author(s) and contributor(s) and not of MDPI and/or the editor(s). MDPI and/or the editor(s) disclaim responsibility for any injury to people or property resulting from any ideas, methods, instructions or products referred to in the content.